Thermal properties of guest-free Si_{136} and Ge_{136} clathrates: A first-principles study

Koushik Biswas,[1,a)] Charles W. Myles,[1] Mahdi Sanati,[1] and G. S. Nolas[2]

[1]*Department of Physics, Texas Tech University, Lubbock, Texas 79409-1051, USA*
[2]*Department of Physics, University of South Florida, Tampa, Florida 33620-5700, USA*

We have used the generalized gradient approximation (GGA) to density functional theory to study the vibrational and thermal properties of guest-free Si_{136} and Ge_{136} clathrates. In order to study the effects of supercell size on our results, we have performed both 34 and 136 atom supercell calculations for each material. We find that the 34 atom supercell calculations predict a small frequency downshift (in comparison with the 136 atom supercell calculations) in the vibrational density of states of both materials. The GGA-predicted Γ phonon frequency of Si_{136} (480 cm^{-1} at $T=0$ K) obtained from the 136 atom calculations is in very good agreement with the experimental value for Na_1Si_{136} (484 cm^{-1} at $T=300$ K). Using the results from our 136 atom calculations, we have also calculated the temperature dependence of the vibrational contributions to the Helmholtz free energy, the entropy, and the specific heat (C_V) of the guest-free Si_{136} and Ge_{136} clathrates. The predicted and experimental heat capacities of Si_{136} are found to be in close agreement. © *2008 American Institute of Physics*. [DOI: 10.1063/1.2960580]

I. INTRODUCTION

In the 1960s, Kasper *et al.* reported the synthesis of two clathrate phases composed of group-I and group-IV elements, Na_8Si_{46} and $Na_xSi_{136}(x<11)$.[1] These materials have crystal structures similar to the well known clathrate hydrates.[2] Since those first reports, there has been considerable interest in these open framework, higher energy crystalline phases of Si and Ge.[3] The continued interest in these materials and related compounds is due both to their electrical properties, which range from metallic behavior to large band gap semiconductors,[3–5] and also due to their glasslike thermal conductivity.[6,7] These characteristics have potential applications in semiconductor and thermoelectric devices. Superconductivity has also been reported in some of the clathrates.[8,9]

Of the two main clathrate phases, there have been fewer investigations of materials of the type-II variety than for the type-I materials. The primitive cell of the type-II structure is face centered cubic and consists of 34 tetrahedrally bonded framework atoms. The larger cubic unit cell contains 136 atoms. The crystal structure is comprised of two different face sharing polyhedra: 28 atom hexakaidecahedra and 20 atom pentagonal dodecahedra, arranged periodically in a 1:2 ratio, respectively.[10]

The type-II clathrates may be represented by the general formula $A_8B_{16}X_{136}$, where A and B are typically group-I or group-II impurity (or "guest") atoms, which fill up the 24 polyhedra (cages) in the 136 atom unit cell. Here, X represents a group-IV atom, Si, Ge, or Sn. However, the site occupancies of the A and B type atoms may be less than 8 and 16, respectively. Gryko *et al.*[11] have reported the synthesis of guest-free Si_{136} (henceforth referred as Si_{136}) by controlled

removal of Na from Na_xSi_{136}. More recently, Guloy *et al.*[12] have reported high yield synthesis techniques of guest-free Ge_{136} (henceforth referred as Ge_{136}). These are important advances, especially in light of the potential applications of these materials in the areas of thermoelectrics and wide band gap semiconductors.

Most of the recent experimental work on type-II Si and Ge clathrates has concentrated on the structural and transport properties.[13,14] Several theoretical studies of the electronic and vibrational properties of filled and guest-free type-II clathrates also exist in the literature.[15–18] Theoretical studies of the thermal properties of these materials have been limited.[19–23] Moriguchi *et al.*[19] have investigated the thermal properties of Si clathrates using the empirical Tersoff potential.[24] Using first-principles-based calculations, Tang *et al.*[20] have reported calculations of the entropy, specific heat capacity, and thermal expansion coefficient of Si_{136}. Experimental work on the specific heat and thermal conductivity of Si_{136} has also been reported by Nolas *et al.*[21] To our knowledge, calculations of the thermal properties of Ge_{136} have not yet been reported.

In this work, we report the results of calculations of the vibrational and thermal properties of Si_{136} and Ge_{136}. The lattice vibrational frequencies have been calculated from first principles at $T=0$ K. We have used these results to predict the temperature dependence of the vibrational contributions to the entropy and specific heat at constant volume (C_V) of Si_{136} and Ge_{136}. The predicted C_V of Si_{136} is found to be in good agreement with experimental specific heat measurements at constant pressure (C_P).

II. THEORETICAL APPROACH

We have used first-principles theoretical methods that are based on the generalized gradient approximation (GGA) to density functional theory. The calculations were per-

---

a)Present address: National Renewable Energy Laboratory, 1617 Cole Blvd., Golden, CO 80401. Electronic mail: koushik_biswas@nrel.gov.

TABLE I. Calculated and experimental (Refs. 11, 12, 21, 30, and 31) crystal parameters and zone-center phonons of Si_{136} and Ge_{136}. Numbers in parentheses were obtained from the 34 atom face centered cubic supercell calculations.

	Lattice parameter (Å)		Bulk modulus (GPa)		Γ phonon (cm^{-1})
	Theory	Expt.	Theory	Expt.	
Si_{136}	14.7043 (14.7049)	14.6260	77.76 (72.8)	90.0	480 (469)
Ge_{136}	15.4432 (15.5088)	15.2115	53.04 (51.4)		278 (263)

formed with the Vienna *ab initio* simulation package (VASP) (Ref. 25) using planewave basis sets and ultrasoft pseudopotentials.[26] The exchange-correlation potential used was that of Perdew *et al.*[27] Large supercell models are necessary to carry out such calculations. In order to study the effect of supercell size on our results, we have performed some of our calculations using both 34 and 136 atom supercells for each clathrate and have compared the results. The predicted thermal properties reported here are based on the 136 atom supercell calculations.

First, we have optimized the material geometry using a $4 \times 4 \times 4$ Monkhorst–Pack k-point grid,[28] with a plane-wave cutoff energy of 600 eV. During this optimization, the different force components were converged to within 0.3 meV/Å or less.

The vibrational calculations were carried out within the harmonic approximation. First, we have obtained the force constant matrix by moving each atom of the relaxed structure by a small finite displacement, $\pm U_0(0.02 \text{ Å})$. VASP allows the determination of the force constant matrix by calculating the Hessian matrix (matrix obtained from the second derivatives of energy with respect to the atomic positions). We have used a $2 \times 2 \times 2$ k-point grid to calculate the Γ-point phonon modes. The dynamical matrix is obtained from the Fourier transform of the force constant matrix. Diagonalization of the dynamical matrix yields the eigenfrequencies and the eigenvectors.[15]

The thermal properties have been evaluated by calculating the Helmholtz free energy. In the harmonic approximation, the vibrational contribution to the Helmholtz free energy is given by[29]

$$F_{\text{vib}}(T) = k_B T \int_0^\infty \left[\frac{1}{2}\hbar\omega + k_B T \ln(1 - e^{-\hbar\omega/k_B T}) \right] g(\omega) d\omega,$$

(1)

where k_B is the Boltzmann constant, $\hbar$ is the Planck constant, and $g(\omega)$ is the vibrational density of states (VDOS). Here, $g(\omega)$ is normalized such that $\int g(\omega)d\omega = 3N$, where N is the number of atoms. The vibrational entropy is given by

$$S_{\text{vib}} = -\left(\frac{\partial F_{\text{vib}}}{\partial T} \right)_V$$

$$= k_B \int_0^\infty \left[\frac{\hbar\omega}{k_B T} (e^{\hbar\omega/k_B T} - 1)^{-1} - \ln(1 - e^{-\hbar\omega/k_B T}) \right] g(\omega) d\omega.$$

(2)

The specific heat at constant volume is calculated using the relation

$$C_V = -T \left(\frac{\partial^2 F_{\text{vib}}}{\partial T^2} \right)_V = T \left(\frac{\partial S}{\partial T} \right)_V.$$

(3)

III. RESULTS AND DISCUSSION

Our calculated lattice parameter, bulk modulus, and Γ phonon frequency for both the Si_{136} and Ge_{136} clathrates are listed in Table I. Available experimental values[12,21,30,31] are also listed there. The calculated lattice parameters are in good agreement with those from experiment. As mentioned earlier, to study the effects of supercell size on our results, we have calculated these properties using both 34 and 136 atom supercell models for the materials. In comparison with the 136 atom supercell calculations, we find that the 34 atom supercell calculations predict smaller Γ phonon frequencies in both materials. Mélinon *et al.*[32] have measured the phonon DOS of different Si clathrates by inelastic neutron scattering techniques. The reported Γ phonon frequency of their Na_1Si_{136} (containing 0.7% of Na) sample was about 484 cm^{-1}.[32] This is in very good agreement with our (136 atom supercell) calculated value of ∼480 cm^{-1} for Si_{136}.

Figures 1 and 2 show our calculated VDOS for Si_{136} and Ge_{136}, respectively. Both figures show the VDOS obtained both from the 34 atom supercell (dotted curve) and from the 136 atom supercell (solid curve) calculations. The calculated VDOS were smoothed with narrow Gaussians (1 cm^{-1} width) to generate a continuous $g(\omega)$.

The predicted VDOS obtained from the 34 atom and 136 atom supercell calculations for Si_{136} (Fig. 1) are qualitatively similar to each other. There is a broad peak located below about 200 cm^{-1} and two sharp peaks near the top of the spectrum, at approximately 440–480 cm^{-1}. These features of the VDOS are in qualitative agreement with the measured
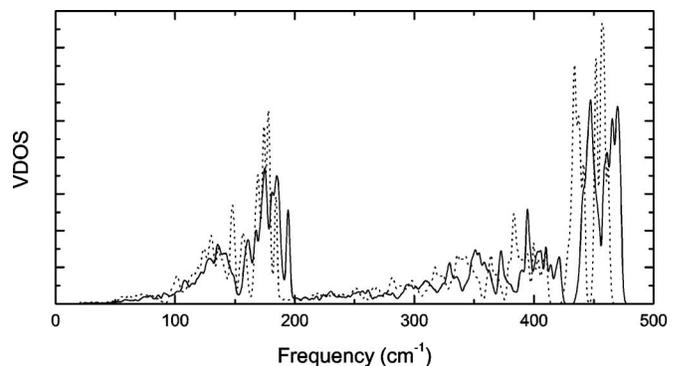

FIG. 1. Calculated VDOS vs frequency for Si_{136} using a 34 atom cell (dotted curve) and a 136 atom cell (solid curve).
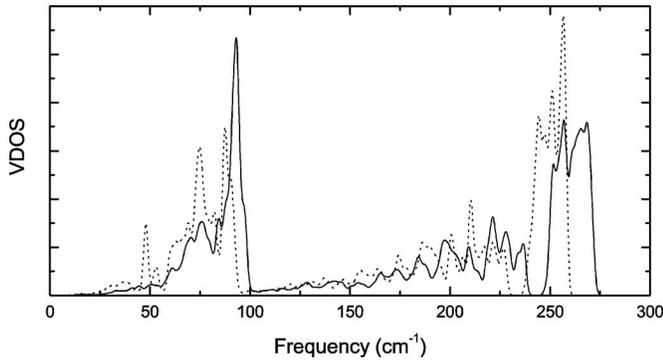
FIG. 2. Calculated VDOS vs frequency for Ge_{136} using a 34 atom cell (dotted curve) and a 136 atom cell (solid curve).

phonon DOS for Na_1Si_{136}.[32] The VDOS peaks obtained from the 34 atom supercell calculations are, however, downshifted by a few wave numbers, compared to the 136 atom calculations. This small frequency shift is observable mostly in the low frequency region (the peaks just below 200 cm^{-1} in Fig. 1), which downshifts the entire spectrum by the same amount. Since VASP uses a direct method for calculating the phonon frequencies (see details in Sec. II), using the larger 136 atom unit cell is an advantage, especially for calculating the low frequency phonons.

The predicted VDOS for Ge_{136} is shown in Fig. 2. For this material, similar to our results for Si_{136}, the 34 atom supercell calculations result in a frequency downshift (of about 10 cm^{-1}) in comparison with the results of the 136 atom calculations. As discussed above, the predicted low frequency phonon modes from the 136 atom supercell calculations are expected to be more accurate than those coming from the 34 atom calculations. The 34 atom calculations also slightly overestimate the Ge–Ge distances (see Table I) in comparison with the 136 atom calculations. This may cause a reduction in the calculated bond-stretching modes in the high frequency region, which likely results in the mentioned downshift. All thermal properties results for both Si_{136} and Ge_{136} discussed in what follows are based on the 136 atom calculations.

Table II shows some of our predicted thermal properties for Si_{136} and Ge_{136}. Recently, Miranda and Antonelli[22] have reported predictions for the Gibbs free energy and the vibrational entropy of the Si_{136} clathrate. Their calculations were based on the reversible scaling Monte Carlo (RS-MC) method.[22] Although a direct comparison between the Helmholtz and Gibbs free energies is not possible, our calculated
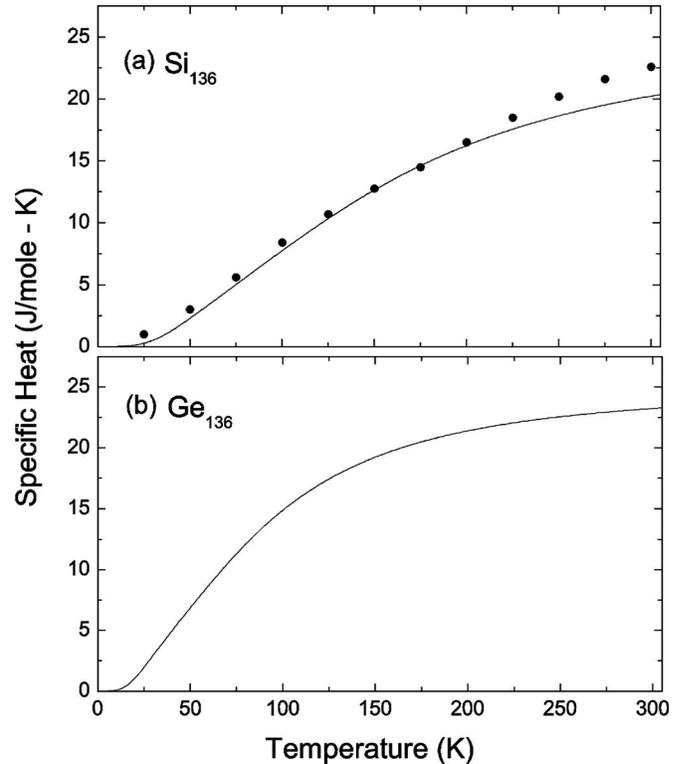

FIG. 3. Predicted temperature dependence of the specific heat at constant volume C_V (solid curves) for Si_{136} (a) and Ge_{136} (b) in the temperature range 0–300 K. Measured isobaric specific heat C_P (discrete symbols) for Si_{136} are shown for comparison.

zero-point energy (ZPE) $F_{vib}(T=0)$ of about 0.059 eV/atom qualitatively agrees with that reported by Miranda and Antonelli (see Fig. 1 in Ref. 22).

The difference between the specific heat at constant pressure C_P and the specific heat at constant volume C_V is given by $C_P - C_V = \alpha^2 T V_{mol} B$,[33] where α is the temperature-dependent volume coefficient of thermal expansion, V_{mol} is the molar volume, and B is the bulk modulus. Because most experiments are conducted at constant pressure, it would be more relevant to calculate the Gibbs free energy.[34] However, the Helmholtz free energy has been calculated in this study. Like most semiconductors, these type-II clathrates are expected to have a low coefficient of thermal expansion. Si_{136}, for example, is reported to have a thermal (linear) expansion coefficient which is less than 4×10^{-6} K^{-1} up to a temperature of about 800 K.[20] Therefore, for this material, the difference between the two specific heats ($C_P - C_V$) should not be too large. Thus, it is appropriate to compare our calculated C_V with the experimental C_P data up to temperatures of 300 K. This same kind of comparison was shown to be appropriate for the specific heats of diamond structured Si and Ge and of wurtzite GaN at temperatures ranging from 0 to 300–400 K.[35,36]

The predicted temperature dependences of C_V (solid curves) for Si_{136} and Ge_{136} in the range 0–300 K are shown in Figs. 3(a) and 3(b), respectively. To our knowledge, there are currently no experimental specific heat data available for Ge_{136}. However, Nolas *et al.*[21] have measured C_P for Si_{136} up to 300 K. Their initial data were not in very good agreement with our calculated C_V values. However, they have recently
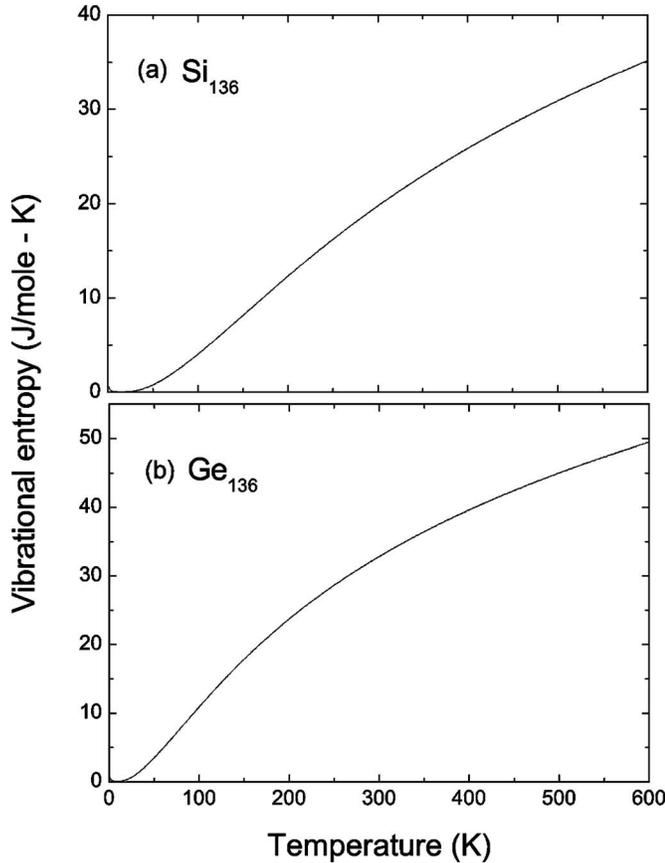
TABLE II. Calculated thermodynamic properties of Si_{136} and Ge_{136}. The specific heat at constant volume C_V at $T=300$ K, the vibrational entropy S_{vib} at $T=300$ K, the ZPE, and the difference of the calculated Helmholtz free energies ΔF_{vib} at $T=0$ and 300 K.

	C_V (J/mole K)	S_{vib} (J/mole K)	ZPE (eV/atom)	ΔF_{vib} (eV/atom)
Si_{136}	20.24	19.77	0.059	−0.0264
Ge_{136}	23.25	32.84	0.033	−0.052

FIG. 4. Predicted temperature dependence of the vibrational entropy for Si_{136} (a) and Ge_{136} (b).

remeasured C_P for Si_{136} (using the same experimental procedure as they described in Ref. 21). Their new data, as shown in Fig. 3(a) (circular points), is in very good agreement with our calculations, up to about 200 K. Above about 200 K, the measured specific heat begins to deviate from the calculated value. Our calculated VDOS at $T=0$ K may be the reason for deviation of the experimental values at higher temperatures. This could also be due to increased anharmonicity of the phonon modes at higher temperatures, whereas the predictions are strictly based on the harmonic approximation.

In order to obtain an estimate of the Debye temperature (θ_D) for Si_{136} and Ge_{136}, we have fitted our calculated value of the specific heat at $T=1$ K with the formula

$$C_V = 9k_B\left(\frac{T}{\theta_D}\right)^3 \int \frac{xe^x}{(e^x-1)^2}dx, \qquad (4)$$

where $x=\hbar\omega/k_B T$ and the integral extends over all ω. This fitting results in predicted values for θ_D of 610 and 341.5 K for Si_{136} and Ge_{136}, respectively.

Figure 4 shows the calculated vibrational entropies of Si_{136} [Fig. 4(a)] and Ge_{136} [Fig. 4(b)] as a function of temperature. Note that Ge_{136} is predicted to have higher vibrational entropy than Si_{136} at all temperatures considered. This is due to the larger contribution to the VDOS that the low frequency vibrational modes in Ge_{136} make than they do in Si_{136}. For example, Fig. 1 shows that the VDOS below about 100 cm^{-1} for Si_{136} is very small. By contrast, in Ge_{136} there is a peak in the VDOS at around 92 cm^{-1}, as can be seen in

Fig. 2. These low frequency modes have longer wavelengths and are associated with larger volumes in configurational space. Therefore, these low frequency modes contribute more toward the vibrational entropy.[36]

Another notable feature of our results is the close proximity of the predicted entropy values of each clathrate with the entropy of their respective diamond phases. The experimental values of the entropy of diamond structured Si and Ge at $T=300$ K are 18.82 and 31.23 J/mole K, respectively.[37] The predicted entropies of both Si_{136} and Ge_{136} at 300 K (shown in Table II) are slightly higher than the values for their corresponding diamond phases. This is expected because the open framework structure of the clathrates should lead to larger entropy.

IV. CONCLUSIONS

We have used first principles GGA-based calculations to study the vibrational and thermal properties of pristine type-II Si_{136} and Ge_{136} clathrates. The vibrational properties were calculated using both 34 and 136 atom supercells. For Si_{136}, the 136 atom calculations predicted a Γ phonon frequency of 480 cm^{-1}. This is in good agreement with the experimental value of 484 cm^{-1} obtained in Na_1Si_{136}.[32] Using the results from our 136 atom calculations, we have calculated the specific heat at constant volume, the vibrational entropy, the ZPE, and the Debye temperature for both clathrates. The temperature dependence of our calculated C_V for Si_{136} is in good agreement with the experimental C_P up to a temperature of about 200 K.

[1] J. S. Kasper, P. Hagenmuller, M. Pouchard, and C. Cros, *Science* **150**, 1713 (1965).
[2] *Water: A Comprehensive Treatise*, edited by F. Franks (Plenum, New York, 1972).
[3] G. S. Nolas, G. A. Slack, and S. B. Schujman, in *Semiconductors and Semimetals*, edited by T. M. Tritt (Academic, San Diego, CA, 2001), Vol. 69, p. 255, and references therein.
[4] N. F. Mott, *J. Solid State Chem.* **6**, 349 (1973).
[5] S. B. Roy, K. E. Sim, and A. D. Caplin, *Philos. Mag. B* **65**, 1445 (1992).
[6] G. A. Slack, in *CRC Handbook of Thermoelectrics*, edited by D. M. Rowe (CRC, Boca Raton, FL, 1995), p. 407.
[7] G. S. Nolas, J. L. Cohn, G. A. Slack, and S. B. Schujman, *Appl. Phys. Lett.* **73**, 178 (1998).
[8] H. Kawaji, H. O. Horie, S. Yamanaka, and M. Ishikawa, *Phys. Rev. Lett.* **74**, 1427 (1995).
[9] D. Connétable, V. Timoshevskii, B. Masenelli, J. Beille, J. Marcus, B. Barbara, A. M. Saitta, G.-M. Rignanese, P. Mélinon, S. Yamanaka, and X. Blasé, *Phys. Rev. Lett.* **91**, 247001 (2003).
[10] G. S. Nolas, J. Sharp, and H. J. Goldsmid, *Thermoelectrics: Basic Principles and New Materials Development* (Springer, New York, 2001).
[11] J. Gryko, P. F. McMillan, R. F. Marzke, G. K. Ramachandran, D. Patton, S. K. Deb, and O. F. Sankey, *Phys. Rev. B* **62**, R7707 (2000).
[12] A. M. Guloy, R. Ramlau, Z. Tang, W. Schnelle, M. Baitinger, and Y. Grin, *Nature (London)* **443**, 320 (2006).
[13] S. Bobev and S. C. Sevov, *J. Solid State Chem.* **153**, 92 (2000).
[14] G. S. Nolas, D. G. Vanderveer, A. P. Wilkinson, and J. L. Cohn, *J. Appl. Phys.* **91**, 8970 (2002).
[15] J. Dong, O. F. Sankey, and G. Kern, *Phys. Rev. B* **60**, 950 (1999).

[16] J. Dong and O. F. Sankey, J. Phys.: Condens. Matter **11**, 6129 (1999).

[17] K. Biswas and C. W. Myles, Phys. Rev. B **74**, 115113 (2006).

[18] K. Biswas and C. W. Myles, Phys. Rev. B **75**, 245205 (2007); K. Biswas and C. W. Myles, J. Phys.: Condens. Matter **19**, 466206 (2007).

[19] K. Moriguchi, S. Munetoh, A. Shintani, and T. Motooka, Phys. Rev. B **64**, 195409 (2001).

[20] X. Tang, J. Dong, P. Hutchins, O. Shebanova, J. Gryko, P. Barnes, J. K. Cockcroft, M. Vickers, and P. F. McMillan, Phys. Rev. B **74**, 014109 (2006).

[21] G. S. Nolas, M. Beekman, J. Gryko, G. A. Lamberton, Jr., T. M. Tritt, and P. F. McMillan, Appl. Phys. Lett. **82**, 910 (2003).

[22] C. R. Miranda and A. Antonelli, Phys. Rev. B **74**, 153203 (2006). References for RS-MC method may be found in this paper.

[23] K. Biswas, Ph.D. thesis, Texas Tech University, 2007.

[24] J. Tersoff, Phys. Rev. B **39**, 5566 (1989); J. Tersoff, Phys. Rev. Lett. **56**, 632 (1986); J. Tersoff, Phys. Rev. B **37**, 6991 (1988); J. Tersoff, *ibid.* **38**, 9902 (1988); J. Tersoff, Phys. Rev. Lett. **61**, 2879 (1988); J. Tersoff, *ibid.* **64**, 1757 (1990); J. Tersoff, Phys. Rev. B **49**, 16349 (1994).

[25] G. Kresse and J. Fürthmuller, Comput. Mater. Sci. **6**, 15 (1996); G. Kresse and J. Hafner, Phys. Rev. B **47**, 558 (1993); G. Kresse and J. Fürthmuller, *ibid.* **54**, 11169 (1996).

[26] D. Vanderbilt, Phys. Rev. B **41**, 7892 (1990); K. Laasonen, R. Car, C. Lee, and D. Vanderbilt, *ibid.* **43**, 6796 (1991); K. Laasonen, A. Pasquarello, R. Car, C. Lee, and D. Vanderbilt, *ibid.* **47**, 10142 (1993).

[27] J. P. Perdew, J. A. Chevary, S. H. Vosko, K. A. Jackson, M. R. Pederson, D. J. Singh, and C. Fiolhais, Phys. Rev. B **46**, 6671 (1992).

[28] H. J. Monkhorst and J. D. Pack, Phys. Rev. B **13**, 5188 (1976).

[29] A. A. Maradudin, E. W. Montroll, G. H. Weiss, and I. P. Ipatova, *Theory of Lattice Dynamics in the Harmonic Approximation* (Academic, New York, 1971).

[30] A. San-Miguel, P. Kéghélian, X. Blase, P. Mélinon, A. Perez, J. P. Itié, A. Polian, E. Reny, C. Cros, and M. Pouchard, Phys. Rev. Lett. **83**, 5290 (1999).

[31] G. K. Ramachandran, P. F. McMillan, S. K. Deb, M. Somayazulu, J. Gryko, J. Dong, and O. F. Sankey, J. Phys.: Condens. Matter **12**, 4013 (2000).

[32] P. Mélinon, P. Kéghélian, A. Perez, B. Champagnon, Y. Guyot, L. Saviot, E. Reny, C. Cros, M. Pouchard, and A. J. Dianoux, Phys. Rev. B **59**, 10099 (1999).

[33] N. W. Ashcroft and N. D. Mermin, *Solid State Physics* (Saunders, Philadelphia, 1976).

[34] For a constant pressure process, $C_P = -T(\partial^2 G/\partial T^2)_P$, where G is the Gibbs free energy. Here we calculate the Helmholtz free energy (F). The two are connected by the relation, $G = F + PV$.

[35] R. K. Kremer, M. Cardona, E. Schmitt, J. Blumm, S. K. Estreicher, M. Sanati, M. Bockowski, I. Grzegory, T. Suski, and A. Jezowski, Phys. Rev. B **72**, 075209 (2005).

[36] S. K. Estreicher, M. Sanati, D. West, and F. Ruymgaart, Phys. Rev. B **70**, 125209 (2004).

[37] I. Barin and O. Knacke, *Thermochemical Properties of Inorganic Substances* (Springer-Verlag, Berlin, 1973).